Arginine-Rich Peptides Destabilize the Plasma Membrane, Consistent with a Pore Formation Translocation Mechanism of Cell-Penetrating Peptides

H. D. Herce,[†‡] A. E. Garcia,[†‡*] J. Litt,[‡§] R. S. Kane,[‡§] P. Martin,[¶] N. Enrique,[¶] A. Rebolledo,[¶] and V. Milesi[¶]
[†]Department of Physics, Applied Physics and Astronomy, [‡]Center for Biotechnology and Interdisciplinary Studies, and [§]Department of Chemical and Biological Engineering, Rensselaer Polytechnic Institute, Troy, New York; and [¶]Universidad Nacional de La Plata, Consejo Nacional de Investigaciones Científicas y Técnicas, La Plata, Argentina

ABSTRACT Recent molecular-dynamics simulations have suggested that the arginine-rich HIV Tat peptides translocate by destabilizing and inducing transient pores in phospholipid bilayers. In this pathway for peptide translocation, Arg residues play a fundamental role not only in the binding of the peptide to the surface of the membrane, but also in the destabilization and nucleation of transient pores across the bilayer. Here we present a molecular-dynamics simulation of a peptide composed of nine Args (Arg-9) that shows that this peptide follows the same translocation pathway previously found for the Tat peptide. We test experimentally the hypothesis that transient pores open by measuring ionic currents across phospholipid bilayers and cell membranes through the pores induced by Arg-9 peptides. We find that Arg-9 peptides, in the presence of an electrostatic potential gradient, induce ionic currents across planar phospholipid bilayers, as well as in cultured osteosarcoma cells and human smooth muscle cells. Our results suggest that the mechanism of action of Arg-9 peptides involves the creation of transient pores in lipid bilayers and cell membranes.

INTRODUCTION

Cell-penetrating peptides (CPPs) are short sequences of amino acids (<30) that are capable of entering most mammalian cells. CPPs have the special property of carrying with them cargoes of a wide range of molecular sizes, such as proteins, oligonucleotides, and even 200 nm liposomes (1–7). Many CPPs are highly cationic and hydrophilic, and exhibit no or relatively low amphipathicity when compared with other peptides that are known to interact with and permeabilize phospholipid membranes. The translocation mechanism by which these peptides are able to enter cells has remained elusive since they were first discovered (1,2,8,9). There is ample evidence suggesting that the uptake is independent of metabolic energy and does not involve any specific cell receptor (2). Other reports indicate that the uptake may involve lipid raft-mediated endocytotic pathways (10–12). Even when the uptake initially follows an endocytotic pathway, arg-rich CPPs are still able to breach the endosome membrane barrier to reach, for example, the cell nucleus (13).

A common feature of cationic CPPs is that they form a rapid and tight interaction with extracellular glycosaminoglycans, such as heparan sulfate, heparin, and chondroitin sulfate B (13). However, whereas a significant part of the uptake of CPPs might involve heparan sulfate receptors, efficient internalization is observed even in their absence (14). Furthermore, these peptides are capable of entering giant unilamellar vesicles (GUVs) composed of model phospholipid membranes (15–18). These results suggest that these peptides can directly interact with the phospholipid bilayer, altering its resting structure, and that these changes facilitate peptide translocation. Taken together, these findings suggest that the binding of highly cationic CPPs to anionic plasma membrane components, such as phosphate groups, could be an important step for effective peptide translocation across a phospholipid bilayer or the cell membrane.

The relevance of peptide-phosphate interactions can be understood through a theoretical model that we recently proposed for the translocation of the Tat peptide (19). This model shows how these peptides may be able to nucleate a pore and diffuse across a phospholipid bilayer. It also highlights the special importance of the charged amino acids in the translocation mechanism, where the Arg and Lys side chains initially bind to the phospholipid phosphate groups, producing strong distortions to the bilayer relative to their resting structure that lead to the formation of a pore. The relevance of the Arg-phosphate interaction has been highlighted in several reports indicating, for example, that poly-Arg peptides translocate more efficiently than poly-Lys peptides and the Tat peptide (9,20). The interaction of Arg amino acids with phosphate groups of the plasma membrane plays a fundamental role in other physiological processes, such as the voltage gating of potassium ion channels (21,22). It has been suggested that the use of Arg in voltage sensors may be an adaptation to the phospholipid composition of cell membranes (23). The importance of guanidinium-phospholipid interactions has also led to intense theoretical research (24–28).

Several Arg-rich antimicrobial peptides can also disrupt and form pores in lipid bilayers and bacterial cell membranes (29–31). It is known that antimicrobial peptides are able to

Submitted January 26, 2009, and accepted for publication May 29, 2009.

*Correspondence: angel@rpi.edu

Editor: Benoit Roux.

0006-3495/09/10/1917/9 $2.00

doi: 10.1016/j.bpj.2009.05.066

translocate across the bacterial plasma membrane in an energy-independent manner. Since CPPs also seem to be capable of translocating in an energy-independent manner, they could share a similar pore-opening mechanism (2,19, 32,33). However, an important difference between hydrophilic CPPs and antimicrobial peptides is the lack of hydrophobic residues in the former case. It has been shown that poly-Arg peptides composed of nine Arg amino acids (Arg-9) are able to translocate across cells very efficiently (34).

Based on the theoretical translocation pathway found for Tat and Arg-9, the central hypothesis of the experimental work presented here is as follows: If Arg-rich CPPs disturb and induce pores in phospholipid membranes, then ions should be able to flow across lipid membranes through these pores. Therefore, applying an electrostatic potential should produce ionic currents through the pores induced by CPPs across phospholipid bilayers and cell membranes. Consistent with this hypothesis, we detected ionic currents induced by Arg-9 on 1), model phospholipid membranes using the planar phospholipid bilayers method (35); and 2), on freshly isolated human umbilical artery (HUA) smooth muscle cells and on cultured osteosarcoma cells using the patch-clamp technique (36). We found that the ionic permeability of phospholipid bilayers and cell membranes is increased by the presence of the Arg-9 peptides. We also explored other peptides and solution conditions that alter this permeability.

This work covers systems with different degrees of complexity, ranging from simulations of very simple systems to experiments on live mammalian cells. The molecular dynamics (MD) studies reported previously for Tat peptides (19) and here for Arg-9 peptides were conducted on simple systems containing a single phospholipid (1,2-dioleoyl-*sn*-glycero-3-phosphocholine (DOPC)), a few peptides, and water. Cell membranes and model membranes are usually composed of multiple lipids (33,37) and modified lipids. Here, we experimentally study a series of systems that are as simple as the systems modeled computationally, systems that contain lipid mixtures containing 1,2-Dioleoyl-*sn*-Glycero-3-[Phospho-*rac*-(1-glycerol)] (DOPG) (e.g., 3:1 DOPC/DOPG), and mammalian cells under different salt and pH conditions. This allows us to present physical, chemical, and biological details of the interactions between Arg-rich peptides and the cell membrane that we believe are essential to unveil the cell translocation pathway for CPPs.

MATERIALS AND METHODS

MD simulations

MD simulations were performed to study the translocation mechanism of Arg-9 peptides across model membranes. The Arg-9 peptides were placed in a periodically repeating box containing water molecules and a preequilibrated lipid membrane composed of DOPC lipids (38,39). The peptides were placed near one side of the bilayer such that the Arg-9 peptides would bind mostly to one layer of the bilayer. These configurations are away from equilibrium. We explored how the systems relax from these configurations. Due to periodic boundary conditions, there are two paths by which an Arg-9 peptide on one layer can move to bind the other layer: one that requires translocation, and one that requires detachment from a lipid layer and diffusion of the Arg-9 peptide from the initial configuration near the water-bilayer boundary on one layer to the other layer. Our calculations include a large number of water molecules such that binding to the proximal layer, given the initial conditions that we selected, is favored. We assume that the Arg-9 peptide remains fully charged throughout the simulation, consistent with observations describing a lack of changes in the pKa of buried Arg side chains in the interior of proteins. Potential of mean force calculations have shown that a single Arg side chain may adopt the protonated state in a lipid bilayer (26,40,41). MacCallum et al. (40) found that the cost of inserting a second charged amino acid side chain into a lipid bilayer is much less than for the first, and therefore it is reasonable for us to assume that Arg-9 will remain fully charged. The total length of the simulation was 500 ns. All simulations were performed using the GROMACS package (42). The simulated system consists of four Arg-9 peptides, 92 DOPC phospholipid molecules, and 8795 water molecules. More details are provided in the Supporting Material.

The experimental techniques included planar lipid bilayers, with bilayers composed of 100% DOPC and 3:1 DOPC/DOPG lipid mixtures. Patch-clamp measurements were conducted in cultured osteosarcoma cells and human smooth muscle cells freshly isolated from the umbilical artery. All experiments measured currents in the presence and absence of Arg-9 peptides and DAP-9 peptides under various conditions. The experimental methods are described in more detail in the Supporting Material.

RESULTS AND DISCUSSION

Theoretical model

We recently proposed a model for the translocation of the HIV-1 Tat peptide based on MD simulations (19). This model shows how these peptides are able to diffuse across phospholipid bilayers. It consists of four basic steps: 1), the peptides bind to the surface of the bilayer, attracted by the phosphate groups of the phospholipids; 2), as the surface concentration of peptides increases, the arrangement of lipids is strongly distorted compared to that in the resting membrane; 3), an Arg side chain translocates to the distal layer, nucleating the formation of a water pore; and 4), a few peptides translocate by diffusing on the surface of the pore and the pore closes. This model highlights the central role of the Arg amino acids, including their strong attachment to the phosphate groups and their ability to induce strong distortions to the structure of the phospholipid bilayer. It has been reported that Arg-9 peptides internalize more efficiently than Tat peptides. Therefore, a natural question is, do peptides composed entirely of Arg amino acids such as Arg-9 follow a translocation pathway similar to that of the Tat peptide? In Fig. 1 are shown four snapshots extracted from this MD simulation, in which it can be seen that Arg-9 follows the same mechanism previously described for Tat.

During the first 50 ns the Arg-9 peptides bind to the phosphate groups in the proximal layer of the lipid bilayer. The guanidinium groups of the Arg side chains make hydrogen-bond contacts with various oxygen atoms of the lipid headgroups, and the peptide is partially immersed into the bilayer at the level of the glycerol groups. After 100 ns an Arg side

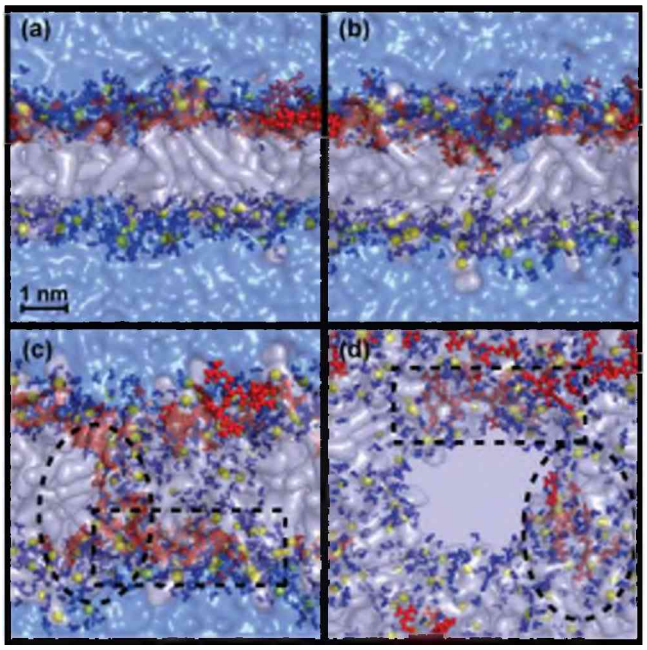

FIGURE 1 Four snapshots of an MD simulation. (*a*) Lateral view showing how the peptides are bound to the membrane before translocation. (*b*) Translocation of an Arg amino acid surrounded by water molecules that nucleates the formation of a water pore. (*c*) Lateral view of the pore, translocated peptide surrounded by a dotted square line, and a translocating peptide circled by an oval dotted line. (*d*) Top view of the pore. The phospholipid molecules are represented with transparent white surfaces, the phosphate atoms are in yellow spheres, the peptide molecules are in red, any water molecule at a distance of <0.35 nm from any phospholipids or amino acid atom is colored in solid blue, and the rest of the water molecules appear as a transparent blue surface.

chain is attracted to a phosphate group in the distal layer of the bilayer. This phosphate group and the Arg side chain carry some water molecules with them, so they are never fully desolvated. During this period of time, a water chain crossing the bilayer is formed and a toroidal pore is nucleated. One of the Arg-9 peptides translocates by diffusing on the surface of the pore. In this calculation, the toroidal pore remains open toward the end of 500 ns. We speculate that the complete translocation of a peptide and closing of the pore will occur on the microsecond timescale; however, this was not explored in our calculations. The radius of the toroidal pore varies in size, having a maximum diameter of 2.5 nm. The pore surface is lined up with phosphate headgroups. The mechanism of Arg side-chain insertion and pore formation observed in the calculations with Arg-9 is identical to the mechanism found for the Tat peptide (19).

The destabilization of lipid membranes and the formation of pores induced by these peptides should lead to an increase in the ionic permeability of phospholipid bilayers and the cell membrane. To validate this prediction of the model, we experimentally investigated the permeabilizing effects of Arg-9 in planar lipid membranes and mammalian cells using two electrophysiological setups as described below.

Permeabilization of model lipid membranes

If CPPs are able to destabilize phospholipid bilayers, producing transient pores across them, then ionic permeabilization should be observed. To test this hypothesis on model lipid membranes, we made phospholipid bilayers using the planar lipid bilayer (also known as the black lipid membrane) method (35). The basic idea of this setup is described in Fig. S1. The addition of micromolar concentrations of Arg-9 to the aqueous solution bathing a planar bilayer membrane led to an increase of membrane conductance in all experiments (>50 experiments). Fig. 2 *a* shows the permeabilization of a phospholipid bilayer composed of a lipid mixture of DOPC/DOPG (3:1) after the addition of Arg-9 at a concentration of 7 μM to the *cis* chamber. After the peptide is added to the *cis* chamber, the ionic permeabilization across the membrane increases. A similar effect is shown in Fig. 2 *c* for bilayers composed entirely of DOPC phospholipid molecules. This proves that anionic phospholipids such as DOPG are not strictly required for peptide permeabilization of the bilayer, since the peptides are still able to interact and permeabilize purely zwitterionic DOPC phospholipid bilayers. The permeabilization increases both continuously and with discrete jumps. The recordings show that the permeability increases and reduces several times until finally the membrane breaks permanently. The transient current spikes were quite abrupt and most of the time did not resemble recordings of well-defined ionic channels, such as voltage-dependent ion channels.

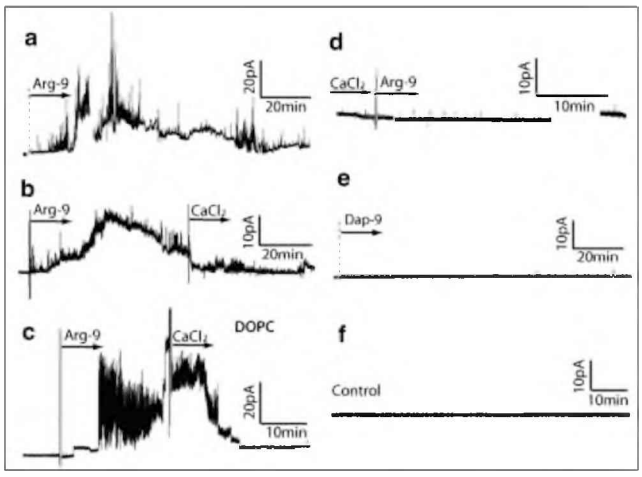

FIGURE 2 Permeabilization of phospholipid bilayers composed of a lipid mixture of DOPC/DOPG (3:1) (*a* and *b*) after the addition of 7μM of Arg-9 to the *cis* chamber, (*c*) phospholipid bilayer composed entirely of DOPC, (*d*) lipid mixture of DOPC/DOPG (the $CaCl_2$ ions are added to the solution before the addition of the peptide), (*e*) control measurement on a lipid mixture of DOPC/DOPG with addition of the Dap-9 peptide, and (*f*) control measurement on a lipid mixture of DOPC/DOPG without peptides. The arrow's origin indicates the time at which the peptides or $CaCl_2$ were added to the solution. The potential of the *cis* chamber relative to the *trans* chamber (the holding potential) is 50 mV. The ionic concentration is 100 mM of KCl and the pH is 7.4.

Positive ions, such as divalent Ca^{2+} ions, would be expected to displace the Arg amino acids or screen the underlying membrane phosphate groups. The permeability of the plasma membrane produced by the peptides should therefore be reduced upon the addition of calcium chloride. Indeed, as shown in Fig. 2 *b*, when calcium chloride was added to the solution, the permeabilization of the membrane reduced to a low baseline level. Moreover, as shown in Fig. 2 *d*, when the peptides were added after the addition of 100 mM of $CaCl_2$ to the solution, there was no increase in the permeability of the bilayer, consistent with the ability of the Ca^{2+} ions to mask the phosphate groups from the peptides. This finding highlights the importance of electrostatic interactions in the initiation of pore formation.

We expect Dap-9 to represent a reasonable negative control peptide. There is substantial experimental evidence indicating that poly-Lys CPPs translocate much less efficiently than poly-Arg CPPs. The MD simulations also suggest that reducing the length of the amino acid side chain will diminish the efficiency of the peptide translocation. Therefore, we tested the effect of Dap-9 (composed of nine 2,3-diaminopropanoic acid residues (Fig. S3)), which has the same charge as Arg-9 but much shorter side chains and amine groups instead of guanidinium groups. As shown in Fig. 2 *e*, Dap-9 does not permeabilize the phospholipid membrane. We also performed a negative control (Fig. 2 *f*) using the same solution but with no peptide addition, and no current increase was observed.

Fig. 3 *a* shows the current induced by Arg-9 across the bilayer for a system with the same composition and held at the same voltage as in Fig. 2 *a*. Fig. 3, *b* and *c*, show the dependence of the current on the voltage. Each interval characterizes a common state observed during the permeabilization of the membrane: control I/V represents a control measurement before the peptide is added, I/V (i) is a measurement after the addition of the peptide but before the steady increase of the conductance across the bilayer, and I/V (ii) is a measurement during the steady increase of conductance across the lipid bilayer. As shown in the figure, current fluctuations were seen initially after the peptides were added, but the baseline current remained unchanged and there was no significant difference in the average current versus voltage recorded (Fig. 3 *b*, I/V (i)) compared to the same measurement obtained before addition of the peptides (Fig. 3 *b*, I/V control). However, after a few minutes the permeabilization became permanent (the current baseline increased) and there was a marked increase in slope of the current versus voltage for I/V (ii) relative to that for control I/V. In Fig. 3, *a* and *c*, it can be seen that after the addition of 100 mM of $CaCl_2$, the permeability decreased. Furthermore, after a period of >100 min, the permeability dropped to very low baseline values, as can be seen in Fig. 3 *c*, I/V (iv).

These results can be interpreted in the following way: After the peptides are added to the solution, they start to bind the bilayer, creating isolated local transient pores across the bilayer. Consequently, the current baseline initially remains at the same level as that before addition of Arg-9. The slope of the current versus voltage plot in I/V (i) remains almost unchanged compared to that for the I/V control, indicating that the permeability increases transiently while the baseline remains unchanged most of the time. After a few minutes, the surface density of membrane-bound peptides increases, destabilizing the membrane more strongly and permanently, as reflected by the increase in the baseline current at I/V (ii) and by the increase in the slope of the current versus voltage. After the addition of $CaCl_2$, the permeability decreases, indicating that Ca^{2+} ions may be competing for phosphate groups and displacing the Arg-9

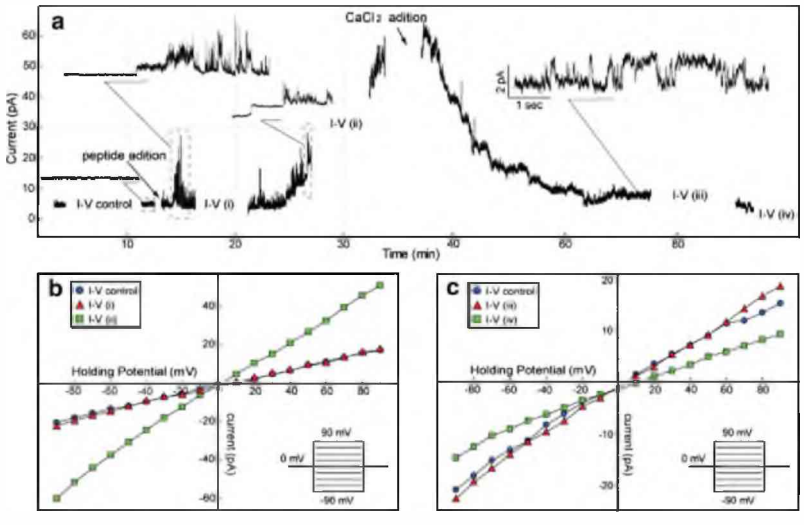

FIGURE 3 Current across a planar lipid bilayer under the same conditions as in Fig. 2, *c* and *d*. (*a*) An average over 10 measurements of current as a function of voltage that were carried out at six different time points: (I/V control) before adding the peptides, (I/V (i)) 10 min after adding the peptide, (I/V (ii)) 40 min after adding the peptide, (I/V (iii)) 30 min after adding $CaCl_2$, and (I/V (iv)) 70 min after adding $CaCl_2$. The inset pictures show amplified sections of the current trace; the scaled time fraction is enclosed by a dotted square, and when time and current are both scaled, the scale is included in the inset picture. (*b* and *c*) Average current as a function of voltage. The voltage is incremented by 10 mV between −90 mV to 90 mv and the potential is held for 150 ms at each voltage. The points in *b* and *c* are the average over 10 consecutive measurements taken at each of the intervals indicated in *a*. It can be seen that after the peptide is added, there are currents jumps before (I/V (i)), but there is not much difference in average between I/V control and (I/V (i)). However, after the permeabilization becomes permanent and the baseline current starts to increase, there is a marked increase in the slope of the current versus voltage (I/V (ii)) relative to the control I/V (I/V control). After addition of $CaCl_2$, the ionic permeabilization reduces. In the last I/V record (I/V (iv)), the current is even lower than the control current. This indicates that $CaCl_2$ reduces the permeability of the membrane to essentially zero.

peptides from the surface of the membrane. This results in the resealing of the phospholipid bilayer.

The insets of Figs. 3 and 4 show amplified current traces. One can see discrete current jumps that resemble the behavior of ion channels in cells, and rapidly fluctuating current jumps that can be clearly distinguished from most ionic channels. The latter types of signals can be used as a footprint to recognize the peptide interaction with the cell membrane, in addition to the expected steady permeabilization increment with time.

Our measurements show that most of the time the current fluctuates rapidly; however, in some cases, more stable current jumps that resemble ion channels can be observed. If we assume that these jumps are associated with the formation of stable pores across the membrane, we can estimate the average radius of these pores by measuring the conductance. To characterize this behavior, we show in Fig. S4 a histogram of the amplitude of those current jumps over 118 events. Assuming that the pore conductivity is equal to that of 100 mM of KCl, we can calculate the pore radius for a conductance G of 4.6 pA/50 mV $= 0.92\ 10^{-10}$ S using $\sigma = Gh/A$, where σ is the conductivity (~1.6 S m^{-1}), A is the area of the pore, G is the conductance (~$0.92\ 10^{-10}$ S), and h is the membrane thickness (~6 nm). The estimated pore diameter for this current value is $d \sim 2\sqrt{(Gh/\sigma\pi)} =$ 0.66 nm, which compares well with the pore diameter observed in the simulations.

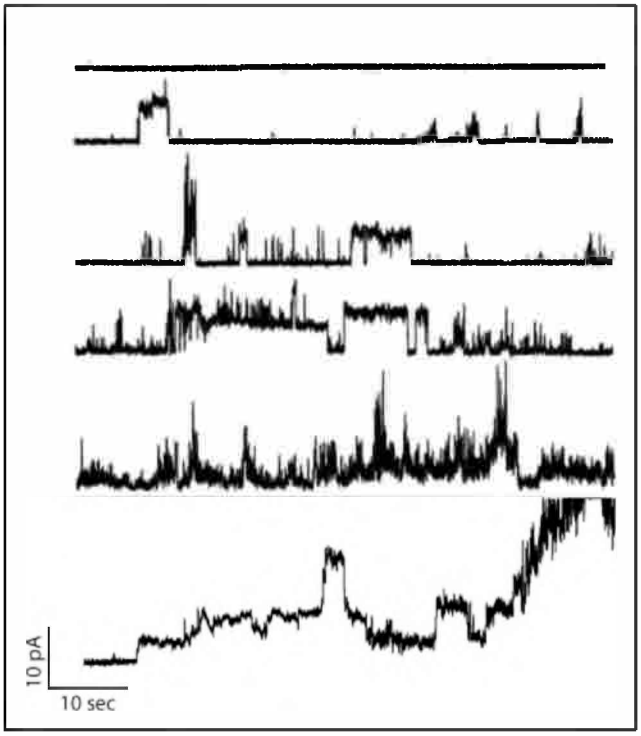

FIGURE 4 Fractions of current traces after the addition of 7μM of Arg-9 to the *cis* chamber as the time progresses. The planar lipid bilayer is composed of a lipid mixture of DOPC/DOPG (3:1). It can be seen that as the time increases, the permeabilization has a noisier trend.

Although Arg-9 is the focus of this experimental work, we are currently investigating the effects of Tat, penetratin, and PG-1. Tat is also a highly hydrophilic CPP, penetratin is a slightly amphiphilic CPP, and PG1 is a pore-forming, Arg-rich, amphiphilic antimicrobial peptide. We also observed in all these cases an increase in the permeabilization of the phospholipid bilayers upon addition to a final concentration of 7 μM (Fig. S5).

Permeability across mammalian cells

The results obtained in lipid bilayers encouraged us to test the peptide's effects on cell membranes of human smooth muscle cells and osteosarcoma cells, although these systems are structurally and functionally much more complex. To accomplish this task, we used the patch-clamp technique in different configurations (whole-cell, cell-attached, and inside-out, as described in the Supporting Material) to measure ionic currents induced by the peptide on the cell membrane.

Whole cell: global permeabilization of the cell

We studied the effects of Arg-9 on isolated HUA smooth muscle cells in the whole-cell configuration (Fig. S2). Fig. 5 *a* shows a typical time course of the current at −50 mV, where we see that the addition of the peptide caused a slow increased in the magnitude of this inward current. The effects of both concentrations of Arg-9 varied among the cells tested, and some of them did not show any significant changes (five out of seven cells tested for 0.07 μM, and two out of nine cells tested for 7 μM). In the cells in which the peptide produced an effect, the average holding current showed a significant increase over the control current measured in the absence of the peptide. The mean current increase induced by 7 μM concentration of Arg-9, expressed as a percentage of the control current, is 126% ± 45% ($n = 7$). We also observed that Arg-9 induced instantaneous current jumps like the ones shown in Fig. 5 *b*. A similar behavior could also be observed at other membrane potentials (data not shown).

It is known that acidification of the extracellular medium can destabilize phospholipid bilayers, thereby enhancing the destabilizing effects induced by the peptide on the plasma membrane. Therefore, we tested the peptide's effect on the holding current at −50 mV in an acid bath solution (pH = 5.5). Under this condition we tested nine HUA smooth muscle cells, and in six of them the current increased to a much greater extent than at the physiological pH of 7.4. The mean current increase (Fig. 5, *c* and *d*) was in this case 460% ± 130% (averaged over six experiments).

Cell-attached and inside-out: local cell permeabilization

We next tested the effect of Arg-9 on cells in the cell-attached and inside-out configurations. These configurations allowed us to measure the currents induced by the peptide in

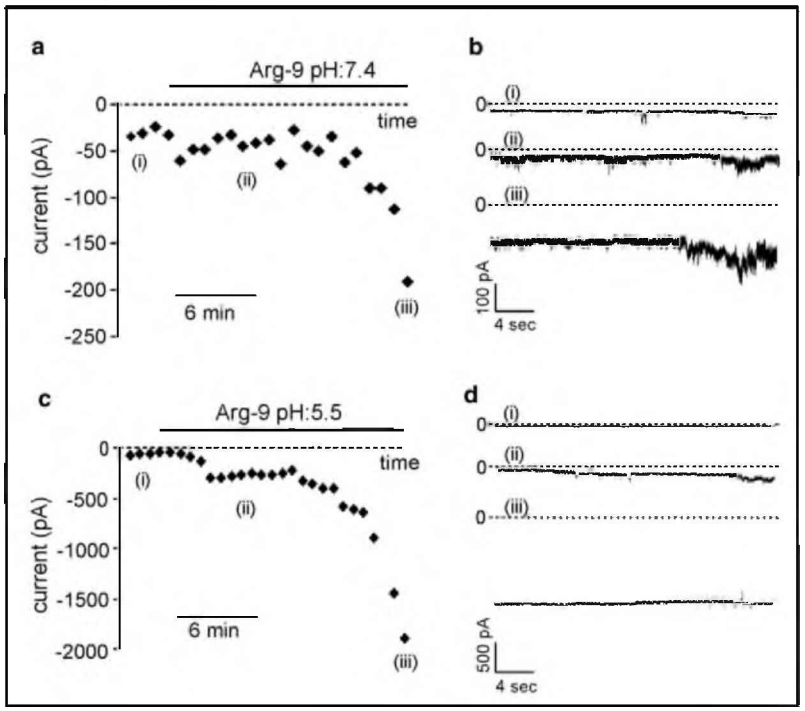

FIGURE 5 (*a*) Time course of the increase of the inward membrane current after the addition of 7 μM of Arg-9 to the extracellular solution in the whole-cell configuration in the case of HUA smooth muscle cells. (*b*) Three typical recordings of this current (pH 7.4), corresponding to the points i, ii, and iii indicated in *a* and *c*. If the pH of the bath solution is lowered to 5.5, the increase in the inward current is more prominent. (*d*) Three typical recordings of this current, corresponding to the points i, ii, and iii indicated in *c*.

membrane areas that are small compared to the whole surface of the cell.

In Fig. 6 we can observe several recordings of the current evoked by a concentration of 7 μM of Arg-9 in the pipette at different times after the seal was obtained in HUA smooth muscle cells. A concentration of 0.07 μM of the peptide was also tested (data not shown), with similar results.

In the majority of tested HUA smooth muscle cells, after periods of time ranging from 10 to 35 min, we began to observe rapidly fluctuating current jumps that resembled the ones we previously observed in artificial phospholipid bilayers. These signals do not follow a repetitive pattern and are difficult to characterize by the typical parameters used to study ionic channels, such as mean current amplitude, open probability, or dwell times. Instead, they resemble the current patterns observed on perturbed membranes of different kinds of cells exposed to mechanical stress (43,44) or in cardiac cells stimulated by photosensitizer-generated reactive oxygen species (45). This characteristic signal can be observed in six out of seven cells obtained from different samples of umbilical cords, although the effect of the peptide is variable in magnitude. We also observed similar rapidly fluctuating current jumps in some of our control cells (without peptide in the pipette), albeit with a much lower frequency of appearance than in the presence of Arg-9. Cell-attached experiments with the peptide (0.07 μM) were also made in UMR106 osteosarcoma cells with similar results.

Fig. 7 shows current snapshots that compare the evolution of current with time for osteosarcoma, HUA smooth muscle cells, and phospholipid bilayers. It can be seen that in every case the ionic currents observed demonstrate a time-increasing, rapidly fluctuating behavior. In the case of the phospholipid bilayer, a stepwise current can also be seen

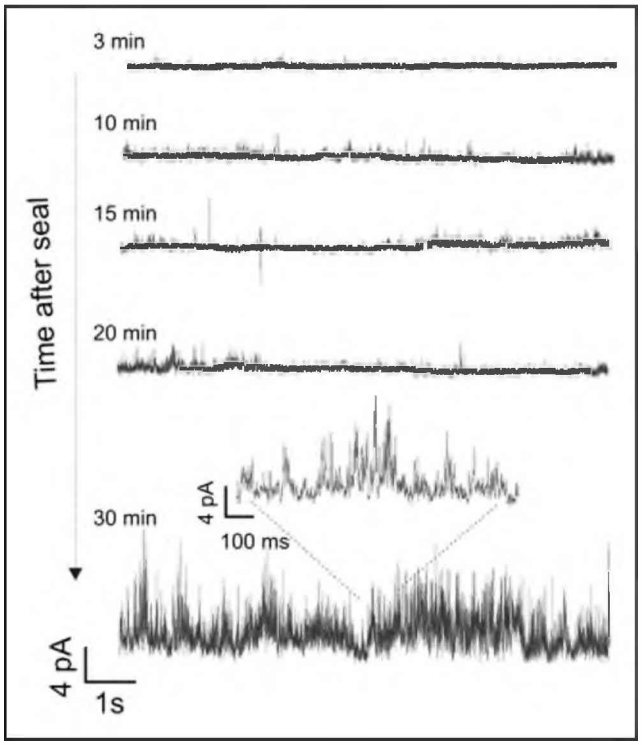

FIGURE 6 Typical cell-attached recordings of the current evoked by the peptide placed inside the pipette in HUA smooth muscle cells at different times after the seal was obtained.

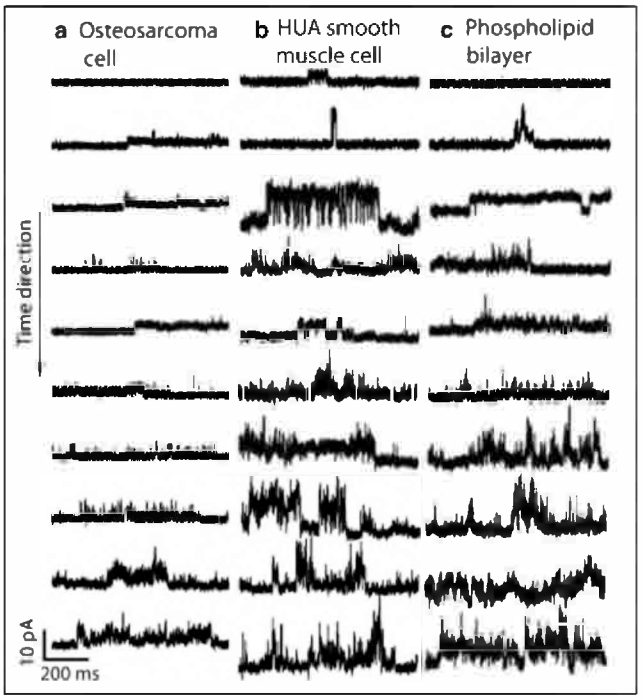

FIGURE 7 Snapshots of typical recordings of the current evoked by the peptide (placed inside the pipette) at different times after the seal was obtained in the cell-attached configuration in (*a*) an osteosarcoma cell, (*b*) an HUA smooth muscle cell, and (*c*) a phospholipid bilayer. It can be seen that as the time increases, the membrane is increasingly permeabilized, and the signal reflects a rapidly fluctuating current in every case.

that resembles the opening behavior of ionic channels. However, if the peptides produce discrete jumps in the cells, these would not be easily distinguished from those belonging to the ion channels already present in the cells. Hence, to minimize the activation of voltage-operated channels, we tested the effects of the peptide using a −50 mV membrane potential at which, in these kinds of cells, most of these voltage-operated ionic channels present a low open probability.

In the inside-out configuration, a micrometer portion of the cell surface was covered by the tip of the glass pipette; it was then was pulled out and only a small piece of the membrane remained in contact with the pipette. In this configuration, the internal surface of the cell membrane was exposed to the bath solution. EGTA (1 mM), a calcium chelator, was used to inhibit the activity of calcium-dependent ionic channels. As in the case of the cell-attached configuration, the recordings were obtained in a symmetric high-potassium saline solution. When a transmembrane potential of −50 mV (outside positive) was applied, a stable holding current appeared. Immediately after the addition of Arg-9 to a concentration of 7 μM to the bath solution (now in contact with the intracellular side of the membrane), the negative net current measured at −50 mV significantly changed reaching more positive current values (Δcurrent = 75 $\pm$ 18 pA, n = 13). After that, we again observed the occurrence of rapidly fluctuating, unstable, variable current jumps, such as those observed in the last part of the recording shown in Fig. 8. These two kinds of behaviors were seen only in the presence of Arg-9 and were similar in all 13 cells tested. They were not observed in the control inside-out patches. The peptide effect seems to have two phases in this patch-clamp configuration: an immediate improvement of seal resistance, followed by an increase of the patch noise, reflecting the destabilizing effect observed in the other configurations. This could be partially explained by the observations made by Chico et al. (46), who reported that significant amounts of poly-D-Arg are retained by plastic and glass surfaces. This finding could explain our results, because Arg-9 would be able to improve the seal by increasing the interaction between the cell membrane and the glass pipette, which is the base of the establishment of a high-resistance seal. This effect does not exclude the fact that Arg-9 can then penetrate by destabilizing the cell membrane, as can be inferred by the occurrence of the typical noisy currents, even though the effective peptide concentration is much less than the 7 μM that is the initial peptide concentration.

CONCLUSIONS

We have shown experimentally that Arg-9 peptides destabilize and permeabilize planar phospholipid bilayers and cell membranes, consistent with our theoretical model.

We performed an MD simulation of Arg-9 that reproduces the main steps for translocation previously observed for the

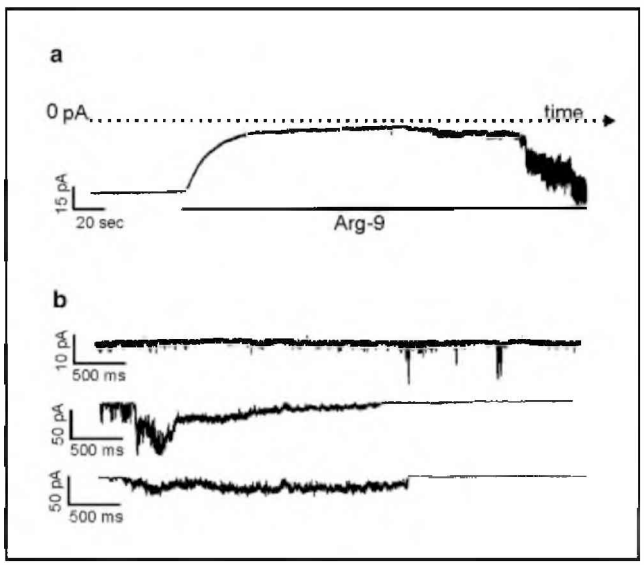

FIGURE 8 Typical recording of Arg-9 effects in an inside-out patch obtained from an HUA smooth muscle cell in symmetrical ionic conditions. (*a*) A recording showing the current measured at 50 mV (outside negative) and its decrease induced by the Arg-9 addition at a concentration of 7 μM. After a few minutes, the current trace becomes rapidly fluctuating in the presence of the peptide. The variability of these current jumps can be observed in the three traces of panel *b* extracted at different time intervals.

Tat peptide (19). The peptides bind to the surface of the bilayer, attracted by the phosphate groups of the phospholipids. The interactions produce large local distortions to the phospholipid bilayer in comparison with its resting structure, and reduce the free-energy barrier as an Arg side chain translocates attracted by phosphate groups on the distal side. This helps the nucleation and the formation of a toroidal pore. Once the pore is formed, the peptides translocate by diffusing on the surface of the pore. The simulations highlight the central role of the Arg side chains in accordance with experimental evidence (47) showing that six or more guanidinium groups are required to efficiently penetrate the cell membranes.

Despite intense research, the details of the cell penetration mechanism of poly-Arg peptides are still under discussion. Futaki and co-workers (48) recently reviewed the subject and concluded that proteoglycans may play a crucial role as primary receptors for peptide internalization, and that both endocytosis and direct membrane translocation are possible entry routes for Arg-rich peptides. Still, some of the most important points that remain to be determined are whether the process is dependent on cell metabolic energy, and whether it requires vesicle formation (i.e., endocytosis (49) and macropinocytosis (50), among others). There is experimental evidence that the uptake of poly-Arg can be inhibited by blocking the cell metabolism with sodium azide (47), lowering the temperature to 4°C (51), or using macropinocytosis and endocytosis inhibitors (11,50,52). However, other reports suggest that cell penetration is independent of metabolic cell energy. For example, knocking down clathrin-mediated and caveolin-mediated endocytosis (53) does not affect the ability of Tat to enter cells. The results presented here can explain the observations of direct translocation of the peptides through a mechanism that is independent of metabolic cell energy.

Our theoretical observations show that Arg-9 is able to nucleate transient pores that would allow ions to flow across it. Therefore, applying an electrostatic potential across the bilayer should induce a net ionic current that could be detected experimentally. We confirmed this prediction by measuring currents across planar phospholipid bilayers and both cultured and freshly isolated mammalian cells.

The electrostatic attraction between the Arg amino acids and the phosphate groups of the membrane is a pivotal step in the translocation model. Therefore, different ions would have a strong effect on the translocation of these peptides if they were able to screen these interactions. If the $CaCl_2$ concentration is increased after addition of the peptides, the permeabilization initiated by Arg-9 will be strongly reduced. We speculate that calcium ions may be competing for the phosphate groups, thereby reducing the binding of the peptides to the surface of the membrane.

We have demonstrated, using theoretical and experimental methods, that a peptide made up entirely of Arg residues is able to interact and permeabilize biological membranes. Furthermore, we have shown that the length of the side chains, and the guanidinium group and ions present can have a profound effect on the ability of these peptides to cross the membrane. Understanding the mechanism by which CPPs disrupt the plasma membrane will contribute to our fundamental knowledge of the mechanisms behind internalization of charged molecules through lipid membranes, and the design of more efficient cargo-carrying molecules, which could lead to better drug-delivery candidates.

SUPPORTING MATERIAL

Methods, references, and five figures are available at http://www.biophysj.org/biophysj/supplemental/S0006-3495(09)01285-5.

We thank L. Rimorini, R. Roldan Palomo, and S. Saleme for discussions and technical assistance with the patch clamp, P. Urdampilleta for collection of the umbilical cords, and Dr. M.S. Molinuevo for the UMR106 osteosarcoma cells.

This study was supported by the National Science Foundation (DMR-0117792), the Nanotoxicology Interdisciplinary Research Team program (CBET 0608978), a National Institute of General Medical Sciences Biomolecular Science and Engineering training program fellowship, and Rensselaer Polytechnic Institute.

REFERENCES

1. Jarver, P., and U. Langel. 2006. Cell-penetrating peptides–a brief introduction. *Biochim. Biophys. Acta.* 1758:260–263.
2. Vives, E., J. P. Richard, C. Rispal, and B. Lebleu. 2003. TAT peptide internalization: seeking the mechanism of entry. *Curr. Protein Pept. Sci.* 4:125–132.
3. Vives, E. 2005. Present and future of cell-penetrating peptide mediated delivery systems: is the Trojan horse too wild to go only to Troy? *J. Control. Release.* 109:77–85.
4. Vives, E., J. Schmidt, and A. Pelegrin. 2008. Cell-penetrating and cell-targeting peptides in drug delivery. *Biochim Biophys Acta.* 1786:126–138.
5. Torchilin, V. P., R. Rammohan, V. Weissig, and T. S. Levchenko. 2001. TAT peptide on the surface of liposomes affords their efficient intracellular delivery even at low temperature and in the presence of metabolic inhibitors. *Proc. Natl. Acad. Sci. USA.* 98:8786–8791.
6. Torchilin, V. P., T. S. Levchenko, R. Rammohan, N. Volodina, B. Papahadjopoulos-Sternberg, et al. 2003. Cell transfection in vitro and in vivo with nontoxic TAT peptide-liposome-DNA complexes. *Proc. Natl. Acad. Sci. USA.* 100:1972–1977.
7. Torchilin, V. P., and T. S. Levchenko. 2003. TAT-liposomes: a novel intracellular drug carrier. *Curr. Protein Pept. Sci.* 4:133–140.
8. Richard, J. P., K. Melikov, E. Vives, C. Ramos, B. Verbeure, et al. 2003. Cell-penetrating peptides. A reevaluation of the mechanism of cellular uptake. *J. Biol. Chem.* 278:585–590.
9. Futaki, S. 2006. Oligoarginine vectors for intracellular delivery: design and cellular-uptake mechanisms. *Biopolymers.* 84:241–249.
10. El-Andaloussi, S., H. J. Johansson, T. Holm, and U. Langel. 2007. A novel cell-penetrating peptide, M918, for efficient delivery of proteins and peptide nucleic acids. *Mol. Ther.* 15:1820–1826.
11. Wadia, J. S., R. V. Stan, and S. F. Dowdy. 2004. Transducible TAT-HA fusogenic peptide enhances escape of TAT-fusion proteins after lipid raft macropinocytosis. *Nat. Med.* 10:310–315.
12. Magzoub, M., A. Pramanik, and A. Graslund. 2005. Modeling the endosomal escape of cell-penetrating peptides: transmembrane pH gradient

driven translocation across phospholipid bilayers. *Biochemistry.* 44:14890–14897.

13. Melikov, K., and L. V. Chernomordik. 2005. Arginine-rich cell penetrating peptides: from endosomal uptake to nuclear delivery. *Cell. Mol. Life Sci.* 62:2739–2749.
14. Richard, J. P., K. Melikov, H. Brooks, P. Prevot, B. Lebleu, et al. 2005. Cellular uptake of unconjugated TAT peptide involves clathrin-dependent endocytosis and heparan sulfate receptors. *J. Biol. Chem.* 280:15300–15306.
15. Binder, H., and G. Lindblom. 2003. Charge-dependent translocation of the Trojan peptide penetratin across lipid membranes. *Biophys. J.* 85:982–995.
16. Persson, D., P. E. Thoren, E. K. Esbjorner, M. Goksor, P. Lincoln, et al. 2004. Vesicle size-dependent translocation of penetratin analogs across lipid membranes. *Biochim. Biophys. Acta.* 1665:142–155.
17. Sharonov, A., and R. M. Hochstrasser. 2007. Single-molecule imaging of the association of the cell-penetrating peptide Pep-1 to model membranes. *Biochemistry.* 46:7963–7972.
18. Terrones, O., B. Antonsson, H. Yamaguchi, H. G. Wang, J. Liu, et al. 2004. Lipidic pore formation by the concerted action of proapoptotic BAX and tBID. *J. Biol. Chem.* 279:30081–30091.
19. Herce, H. D., and A. E. Garcia. 2007. Molecular dynamics simulations suggest a mechanism for translocation of the HIV-1 TAT peptide across lipid membranes. *Proc. Natl. Acad. Sci. USA.* 104:20805–20810.
20. Futaki, S. 2005. Membrane-permeable arginine-rich peptides and the translocation mechanisms. *Adv. Drug Deliv. Rev.* 57:547–558.
21. Hessa, T., H. Kim, K. Bihlmaier, C. Lundin, J. Boekel, et al. 2005. Recognition of transmembrane helices by the endoplasmic reticulum translocon. *Nature.* 433:377–381.
22. Hessa, T., S. H. White, and G. von Heijne. 2005. Membrane insertion of a potassium-channel voltage sensor. *Science.* 307:1427.
23. Schmidt, D., Q. X. Jiang, and R. MacKinnon. 2006. Phospholipids and the origin of cationic gating charges in voltage sensors. *Nature.* 444:775–779.
24. Vorobyov, I., L. Li, and T. W. Allen. 2008. Assessing atomistic and coarse-grained force fields for protein-lipid interactions: the formidable challenge of an ionizable side chain in a membrane. *J. Phys. Chem. B.* 112:9588–9602.
25. MacCallum, J. L., W. F. Bennett, and D. P. Tieleman. 2007. Partitioning of amino acid side chains into lipid bilayers: results from computer simulations and comparison to experiment. *J. Gen. Physiol.* 129:371–377.
26. Yoo, J., and Q. Cui. 2008. Does arginine remain protonated in the lipid membrane? Insights from microscopic pKa calculations. *Biophys. J.* 94:L61–L63.
27. Freites, J. A., D. J. Tobias, G. von Heijne, and S. H. White. 2005. Interface connections of a transmembrane voltage sensor. *Proc. Natl. Acad. Sci. USA.* 102:15059–15064.
28. Roux, B., and K. Schulten. 2004. Computational studies of membrane channels. *Structure.* 12:1343–1351.
29. Oren, Z., and Y. Shai. 1998. Mode of action of linear amphipathic α-helical antimicrobial peptides. *Biopolymers.* 47:451–463.
30. Matsuzaki, K. 1999. Why and how are peptide-lipid interactions utilized for self-defense? Magainins and tachyplesins as archetypes. *Biochim. Biophys. Acta.* 1462:1–10.
31. Tang, M., A. J. Waring, and M. Hong. 2007. Phosphate-mediated arginine insertion into lipid membranes and pore formation by a cationic membrane peptide from solid-state NMR. *J. Am. Chem. Soc.* 129: 11438–11446.
32. Herce, H. D., and A. E. Garcia. 2007. Cell penetrating peptides: how do they do it? *J. Biol. Phys.* 33:345–356.
33. Mishra, A., V. D. Gordon, L. Yang, R. Coridan, and G. C. Wong. 2008. HIV TAT forms pores in membranes by inducing saddle-splay curvature: potential role of bidentate hydrogen bonding. *Angew. Chem. Int. Ed. Engl.* 47:2986–2989.
34. Wender, P. A., D. J. Mitchell, K. Pattabiraman, E. T. Pelkey, L. Steinman, et al. 2000. The design, synthesis, and evaluation of molecules that enable or enhance cellular uptake: peptoid molecular transporters. *Proc. Natl. Acad. Sci. USA.* 97:13003–13008.
35. Mueller, P., D. O. Rudin, H. T. Tien, and W. C. Wescott. 1962. Reconstitution of cell membrane structure in vitro and its transformation into an excitable system. *Nature.* 194:979–980.
36. Hamill, O. P., A. Marty, E. Neher, B. Sakmann, and F. J. Sigworth. 1981. Improved patch-clamp techniques for high-resolution current recording from cells and cell-free membrane patches. *Pflugers Arch.* 391:85–100.
37. Bretscher, M. S. 1972. Asymmetrical lipid bilayer structure for biological membranes. *Nat. New Biol.* 236:11–12.
38. Berger, O., O. Edholm, and F. Jahnig. 1997. Molecular dynamics simulations of a fluid bilayer of dipalmitoylphosphatidylcholine at full hydration, constant pressure, and constant temperature. *Biophys. J.* 72:2002–2013.
39. Feller, S. E., D. X. Yin, R. W. Pastor, and A. D. MacKerell. 1997. Molecular dynamics simulation of unsaturated lipid bilayers at low hydration: parameterization and comparison with diffraction studies. *Biophys. J.* 73:2269–2279.
40. MacCallum, J. L., W. F. D. Bennett, and D. P. Tieleman. 2008. Distribution of amino acids in a lipid bilayer from computer simulations. *Biophys. J.* 94:3393–3404.
41. Johansson, A. C. V., and E. Lindahl. 2009. Titratable amino acid solvation in lipid membranes as a function of protonation state. *J. Phys. Chem. B.* 113:245–253.
42. Van Der Spoel, D., E. Lindahl, B. Hess, G. Groenhof, A. E. Mark, et al. 2005. GROMACS: fast, flexible, and free. *J. Comput. Chem.* 26:1701–1718.
43. Patel, A. J., E. Honore, F. Maingret, F. Lesage, M. Fink, et al. 1998. A mammalian two pore domain mechano-gated S-like K+ channel. *EMBO J.* 17:4283–4290.
44. Suchyna, T. M., S. R. Besch, and F. Sachs. 2004. Dynamic regulation of mechanosensitive channels: capacitance used to monitor patch tension in real time. *Phys. Biol.* 1:1–18.
45. Tarr, M., and D. P. Valenzeno. 1998. Photomodification of cardiac membrane: chaotic currents and high conductance states in isolated patches. *Photochem. Photobiol.* 68:353–360.
46. Chico, D. E., R. L. Given, and B. T. Miller. 2003. Binding of cationic cell-permeable peptides to plastic and glass. *Peptides.* 24:3–9.
47. Mitchell, D. J., D. T. Kim, L. Steinman, C. G. Fathman, and J. B. Rothbard. 2000. Polyarginine enters cells more efficiently than other polycationic homopolymers. *J. Pept. Res.* 56:318–325.
48. Futaki, S., I. Nakase, A. Tadokoro, T. Takeuchi, and A. T. Jones. 2007. Arginine-rich peptides and their internalization mechanisms. *Biochem. Soc. Trans.* 35:784–787.
49. Drin, G., S. Cottin, E. Blanc, A. R. Rees, and J. Temsamani. 2003. Studies on the internalization mechanism of cationic cell-penetrating peptides. *J. Biol. Chem.* 278:31192–31201.
50. Khalil, I. A., K. Kogure, S. Futaki, and H. Harashima. 2006. High density of octaarginine stimulates macropinocytosis leading to efficient intracellular trafficking for gene expression. *J. Biol. Chem.* 281:3544–3551.
51. Fretz, M. M., N. A. Penning, S. Al-Taei, S. Futaki, T. Takeuchi, et al. 2007. Temperature-, concentration- and cholesterol-dependent translocation of L- and D-octa-arginine across the plasma and nuclear membrane of CD34+ leukaemia cells. *Biochem. J.* 403:335–342.
52. Meier, O., and U. F. Greber. 2003. Adenovirus endocytosis. *J. Gene Med.* 5:451–462.
53. Ter-Avetisyan, G., G. Tuennemann, D. Nowak, M. Nitschke, A. Herrmann, et al. 2009. Cell entry of arginine-rich peptides is independent of endocytosis. *J. Biol. Chem.* 284:3370–3378.